# ADSORPTION OF POLYACRYLATES ON HEMATITE: *IN SITU* EXAMINATION BY FTIR-ATR AT HIGH AND LOW PH

Fawell, P.D.[2], Kirwan, L.J.[1], van Bronswijk, W.[1]
[1] *AJ Parker Cooperative Research Centre for Hydrometallurgy, Curtin University of Technology, Western Australia*
[2] *AJ Parker Cooperative Research Centre for Hydrometallurgy, CSIRO Minerals, Bentley, Western Australia*

## Abstract

For the majority of tailing substrates, flocculant adsorption proceeds through the interaction of amide functionalities with neutral surface species. For anionic copolymer flocculants, the acrylate component of the polymer does not directly participate in adsorption, only serving to provide chain extension in solution. The flocculation of bauxite residue with high molecular weight polyacrylates represents an almost unique situation, with the absence of amide functionalities implying a totally different adsorption mechanism.

Direct examination of polyacrylate adsorption within the complex matrix of real liquors and the mixture of residue phases is difficult, making it necessary to focus on model substrates (hematite, goethite) and synthetic liquors. Previous spectral studies have suffered from the need to dry solids following adsorption, potentially altering the adsorbed species. This study presents evidence obtained by Fourier Transform Infrared-Horizontal Attenuated Total Reflection (FTIR-ATR), in which liquors of high pH were pumped over a hematite colloid deposited on a zinc selenide crystal. For the first time *in situ* information has been obtained for the adsorbed polymer at the solid-liquid interface under a range of conditions.

Both the adsorbed species and the rate of polymer adsorption differ greatly for adsorption at high and low pH, and the critical role of the solution cation at high pH has been confirmed. Detailed analysis of the FTIR-ATR spectra also allows quantification of the adsorbed flocculant. The adsorption behaviour is discussed in terms of the surface structure and charge at high pH.

## 1 Introduction

### 1.1 *Bauxite residue flocculation*

The Bayer Process for the extraction of alumina from bauxite generates large volumes of residue in alkaline liquors. Solid-liquid separation is typically achieved through flocculation in gravity thickeners, with throughput, underflow density and clarity as critical performance criteria. While there have been significant advances in the nature of flocculants used to treat bauxite residue, comparatively little fundamental research has been carried out to characterise the flocculant adsorption mechanisms. A better understanding of such mechanisms may allow more efficient application of the flocculants and ultimately lead to the development of improved polymer products.

The composition of Bayer residues varies depending on the source of the bauxite and the processing conditions. As hematite ($Fe_2O_3$) is the major phase in most operations, it often has been the primary focus of laboratory-based studies on flocculation behaviour that seek to simplify the potential variables.

High molecular weight polyacrylates are commonly used for the flocculation of bauxite residue. This distinguishes bauxite residue from the majority of other mineral tailings systems, for which the dominant flocculants used are acrylamide homopolymers or copolymers with sodium acrylate. In such systems, the amide functionality provides hydrogen bonding to the mineral, while charge repulsions from carboxylate functionalities along the polymer may serve to extend the dimensions of unadsorbed loops and tails, thereby enhancing the prospects for particle bridging. For the fully hydrolysed polyacrylate flocculants, a different mechanism is clearly required to describe the adsorption process.

Recent studies of flocculant adsorption on hematite have used settling and adsorption properties and atomic force microscopy to obtain indirect information on the process, but do not provide any indication of the surface interactions. Jones et al. utilised infrared spectroscopy to directly study the interaction of carboxylate functionalities with hematite. However, this was achieved by *ex situ* diffuse reflectance (DRIFT), which may lead to potential changes in the nature of the adsorbed species during the washing and drying process. Adsorbed segments may also represent only a small fraction of the total polymer chain length. Polymer tails and loops that were unadsorbed while in solution may collapse onto the surface during drying, distorting the true binding behaviour.

### 1.2 *FTIR-ATR*

Attenuated total internal reflectance (ATR) infrared spectroscopy offers the possibility of *in situ* examinations of the solid-liquid interface without any other sample treatment that may change the surface characteristics. It may be achieved through (i) adsorption directly onto the infrared element (IRE), (ii) adsorption onto particulate matter that is then contacted with the IRE, or (iii) adsorption onto a coated IRE. Adsorption on a coated IRE is perhaps the most versatile option, and allows quantitative surface excess measurements equivalent to those obtained by solution depletion.

Utilising the second approach, Hind et al. have successfully used FTIR-ATR to examine the adsorption of quaternary ammonium compounds on solid sodium oxalate and gibbsite in synthetic Bayer liquors. However, they only used the spectra to estimate the relative amounts of different chain length compounds that adsorbed under

selected conditions. It can be assumed that peak positions in the spectra of their quaternary ammonium compounds were insensitive to the adsorption state, and therefore did not lend themselves to mechanistic interpretation. In contrast, the carboxylate functionality present in polyacrylate flocculants offers considerable potential for adsorbed peak analysis.

### **1.3** *Objectives*

This study sought to establish if FTIR-ATR can effectively distinguish the solid-liquid interface from the bulk liquor for polyacrylate solutions in contact with a deposited hematite layer. Spectra acquired under low and high pH conditions were compared to provide insight into the differing modes of polyacrylate adsorption, and in particular, why the negatively charged polymer is attracted to the hematite surface at high pH. Factors affecting the extent of polyacrylate adsorption at high pH were considered with reference to the expected hematite surface structure.

## 2 Experimental

### **2.1** *Flocculant solutions*

Details of the polymers used in this study are given in Table 1. Each concentrated stock solution (1 000 – 10 000 ppm) was prepared by the addition of powdered polymer to an appropriate aqueous solution followed by gentle mixing for several days to ensure optimal dispersion. The solution was made up to the required pH and ionic strength, then stirred for a further day before recording the final pH. Dilutions were made from these stock solutions when required.

### **2.2** *Hematite colloid preparation and deposition*

An aqueous hematite colloid was prepared by mixing equal volumes of $FeCl_3$ (0.01 M) and HCl (0.004 M) solutions, followed by refluxing for 48 hours. On cooling, the colloid was dialysed against ultra-pure water for 7 days with the water changed daily. The resultant solution was analysed for iron by ICP to determine the colloid concentration and by laser diffraction (Malvern Mastersizer) for the particle size distribution. The colloid was found to have a very narrow distribution, with $d_{10}$, $d_{50}$ and $d_{90}$ of 0.056, 0.096 and 0.152 µm, respectively. The colloid solids were shown by XRD to be pure hematite, while TEM confirmed the particle sizing and that the particles were monoclinic in shape.

A thin layer was formed on the zinc-selenide crystal of the ATR accessory by carefully dispensing 30 µL of the colloid to a diameter of 5 mm and allowing the slurry to dry. Optical and atomic force microscopy of the film confirmed that it was distributed continuously across the ZnSe surface.

### **2.3** *Spectral measurements*

Figure 1 gives a schematic representation of the experimental set-up for ATR measurements and shows that the IR radiation from the incident beam may penetrate a small distance into the solution (the “evanescent wave”). However, the intensity of the wave diminishes rapidly with distance, and therefore the majority of the information received deals with the solid-liquid interface.

Solutions were pumped through the cell at a constant flowrate (1.0 mL $min^{-1}$) using a peristaltic pump, with spectra recorded at regular intervals. Equilibrium was first achieved using the background electrolyte, then the procedure was repeated with solution containing polymer. Concentrated flocculant solution spectra were also acquired with the flowcell in the absence of the hematite colloid layer. FTIR-ATR spectra were obtained using a Bruker IFS 66 instrument, Harrick “Seagull” variable angle ATR accessory and MCT (mercury cadmium telluride) detector, at a resolution of 4 $cm^{-1}$. The number of scans accumulated depended on the intervals between acquiring spectra – 56 and 128 scans were accumulated for intervals of 30 and 60 s, respectively, while 256 scans were accumulated for intervals greater than 60 s. The incident angle of the ATR accessory was set to 45º.

### **2.4** *Surface charge measurements*

Electrophoretic measurements were obtained using a Brookhaven ZetaPlus instrument (through the University of NSW). Measurements were recorded at 23°C using a

Table 1 — Polymers used in this study.

| Polymer | Manufacturer | Molecular Weight | Code |
|---|---|---|---|
| Polyacrylic acid | Aldrich | ~2 000 | PAA2K |
| Polyacrylic acid | Aldrich | ~450 000 | PAA450K |
| Sodium polyacrylate | Ciba Specialty Chemicals | ~13 000 000 | PAA13M |

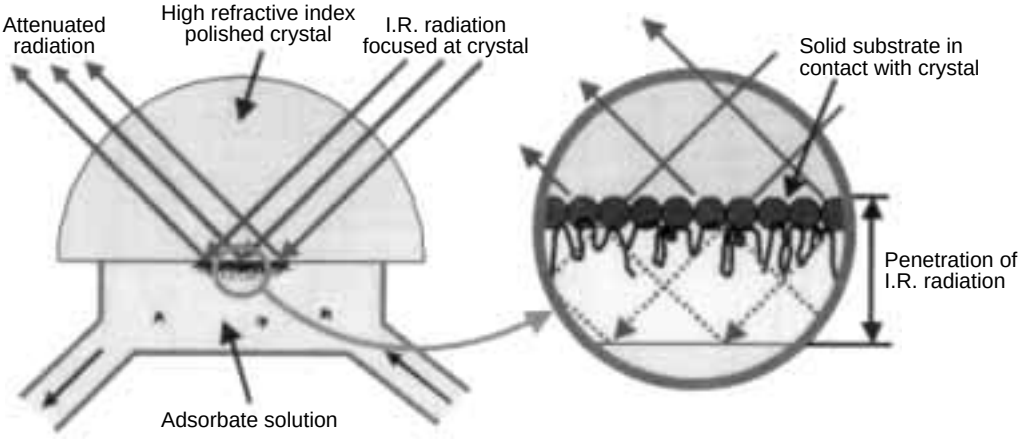


Figure 1 — Schematic representation of the ATR cell, showing the deposited hematite colloid and flocculant adsorbed from the synthetic liquor (applied at a constant flowrate).

voltage of 3 V and a frequency of 2 Hz. A total of three sub-samples were analysed for each sample and the error taken as the standard deviation. Each sub-sample was subject to three analytical runs by the instrument at 5 cycles per run, with the zeta potential calculated using the Smoluchowski model.

The hematite colloid was diluted to a concentration of 30 ppm, with the pH adjusted using an alkali hydroxide solution and the ionic strength using the corresponding alkali nitrate salt (chloride salts could not be used due to reactions with the palladium electrode during zeta potential measurements). Prior to testing, samples were vigorously shaken and then placed in an ultrasonic bath for approximately one minute to aid in particle dispersion.

### **2.5** *Multi-angle laser light scattering (MALLS)*

Static light scattering was carried out with a DAWN DSP photometer (Wyatt Technology) fitted with a K5 flowcell. A 1 wt% dextran solution (0.2 µm filtered) was used for normalisation. PAA450K (200 ppm) was prepared in ultrapure water (0.1 µm filtered) with pH adjusted using the corresponding alkali hydroxide and ionic strength by using the corresponding alkali chloride. Solutions were introduced into the flowcell at 10 mL $h^{-1}$ through a 5 µm filter. Scattering was collected at 15 collimated detectors at fixed angles around the flowcell, and DAWN 3.30 software used to extract the radius of gyration through the Debye method.

## 3 Results and Discussion

### **3.1** *Solution spectra*

Prior to examining polymer adsorption on hematite, the behaviour of the polymers in solution must first be understood. The acrylate functionality of polyacrylate has characteristic absorption bands in the 1000 to 2000 $cm^{-1}$ region of the infrared spectrum. Spectra of concentrated polymer solutions as detected by FTIR-ATR on a clean, uncoated ZnSe crystal were recorded, with Figure 2 showing the main absorption bands of interest for PAA450K at pH 2 and 13. A clear distinction can be made between the peaks for the protonated and unprotonated structures, the latter allowing delocalisation of the charge across the functionality.

These peaks did not shift as the solution concentration was changed, while at pH 13 the peak positions were unaffected by the presence of 1 M NaCl. Very high concentration were required to achieve measurable peaks against the uncoated crystal, and at 100 ppm of polymer or below it was not possible to distinguish any polymer peaks in the spectra.

### **3.2** *Adsorbed species spectra*

Substantially different spectra were observed for polymer solutions after the deposition of colloidal hematite onto the ATR crystal. For 50 ppm PAA450K at pH 2, distinct peaks associated with the polymer were seen to grow steadily, with equilibrium achieved after ~2 hours (Figure 3a). The intensity of these peaks at such a low applied solution concentration indicated polyacrylic acid was attracted to the hematite interface, most likely leading to adsorption. Figure 3b shows that similar behaviour was observed at pH 13, although the peaks were in quite different positions and were only seen under conditions of high ionic strength (the latter is discussed in more detail in Section 3.3). The spectra also suggest that adsorption equilibrium was approached more rapidly at pH 13 than at pH 2.

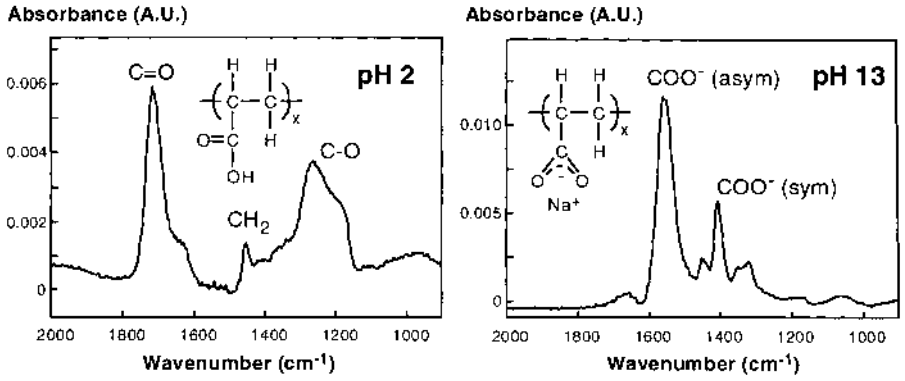


Figure 2 — Spectra of concentrated polyacrylate (PAA450K – 10 000 ppm) in solution at pH 2 and 13.

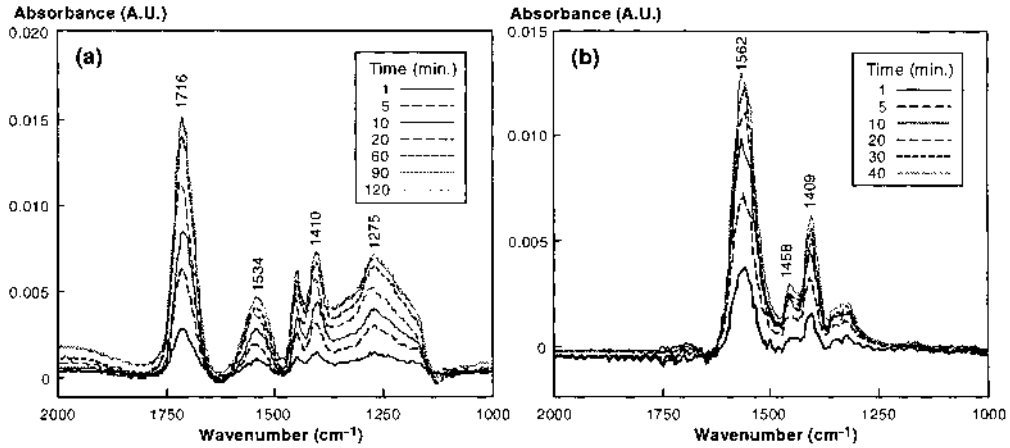


Figure 3 — Spectra of PAA450K (50 ppm) on hematite at (a) pH 2 and (b) pH 13 in 1.0 M NaCl.

Table 2 — Comparison of FTIR-ATR peak assignments for a polyacrylic acid in solution and after adsorption onto colloidal hematite at pH 2 and at pH 13 with 1 M NaCl.

| Conditions | Peak position ($cm^{-1}$) | | Peak |
|---|---|---|---|
| | Solution spectra | Adsorbed spectra | assignments |
| pH 2 | 1717 | 1716 | -C=O |
| | | **1543** | **$-COO^-$ (asymmetric)** |
| | 1455 | 1455 | $CH_2$ scissor |
| | | **1410** | **$-COO^-$ (symmetric)** |
| | 1265 | 1275 | -C-O |
| pH 13 (1 M NaCl) | **1562** | **1562** | **$-COO^-$ (asymmetric)** |
| | 1453 | 1458 | $CH_2$ scissor |
| | **1408** | **1409** | **$-COO^-$ (symmetric)** |

The principle features of these spectra are summarised in Table 2, together with those for the corresponding solution spectra at 10 000 ppm. At pH 2 the solution carboxylate peaks (~1716 and 1275 $cm^{-1}$) may also be seen in the adsorbed species spectra. This is not surprising, as not every functional group on the polymer is expected to adsorb, and numerous unadsorbed groups (parts of polymer loops and tails) are inevitably drawn within the measurement zone following adsorption. Of greater interest are the additional carboxylate stretching vibrations (1410 and 1543 $cm^{-1}$) in the spectra, which form the basis for the interpretation of the adsorption mechanism.

Deacon and Phillips studied the relationship between the carbon-oxygen stretching frequencies of carboxylato complexes and the type of carboxylate coordination. By comparing the difference between the symmetric and asymmetric stretching frequencies of the carboxylate ion ($\Delta\nu$) bound to transition metals to that of the sodium salt, they proposed the set of selection rules, summarised below, for identifying the bonding mechanisms shown in Figure 4:

- If there is C=O character in the spectrum and $\Delta\nu_{(adsorbed)}$ is greater the $\Delta\nu_{(salt)}$ then the adsorbed structure is monodentate (I).
- If there is no C=O character in the spectrum and $\Delta\nu_{(adsorbed)}$ is smaller than $\Delta\nu_{(salt)}$ then the adsorbed structure is bidentate chelating (II).
- If there is no C=O character in the spectrum and $\Delta\nu_{(adsorbed)}$ is similar to $\Delta\nu_{(salt)}$ then the adsorbed structure is bidentate bridging (III).

For the sodium salt of polyacrylic acid in solution, $\Delta\nu_{(salt)}$ was 154 $cm^{-1}$, while $\Delta\nu_{(adsorbed)}$ at pH 2 was significantly lower at 133 $cm^{-1}$. On this basis, an adsorbed species involving bidentate chelation is indicated, similar to structure (II) in Figure 4. The adsorbed polymer on hematite may therefore be represented by Figure 5a, with the constraints of the bidentate chelation making it unlikely that adjacent functionalities would be adsorbed. Similar behaviour was displayed by the different molecular weight polymers PAA2K and PAA13M, although the relative intensities of the solution and adsorbed carboxylate peaks did change with time. The analysis of such variations to estimate the proportion of adsorbed segments will be described in a separate publication.

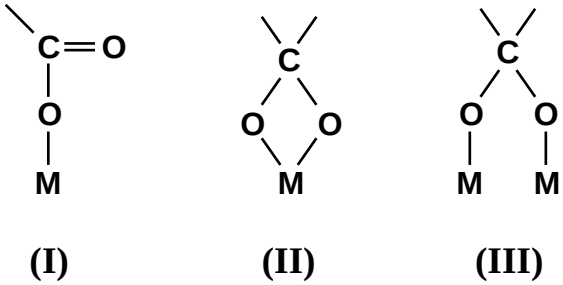


Figure 4 — Modes of carboxylate-metal complexation; monodentate (I), bidentate chelating (II), and bidentate bridging (III).

The adsorbed spectrum for PAA450K at pH 13 with 1 M NaCl was indistinguishable from the solution spectrum obtained at a much higher polymer concentration but in the same electrolyte. It was therefore not possible to discriminate between adsorbed and unadsorbed polymer segments. From Table 2 it can be seen that $\Delta\nu_{(salt)}$ for the sodium salt of polyacrylic acid in solution was almost identical to the $\Delta\nu_{(adsorbed)}$ at pH 13 with 1 M NaCl (154 and 153 $cm^{-1}$, respectively). Use of the Deacon and Phillips selection rules would indicate bidentate bridging onto the surface, but such a structure would not account for the critical role of the solution cation in enabling adsorption. More

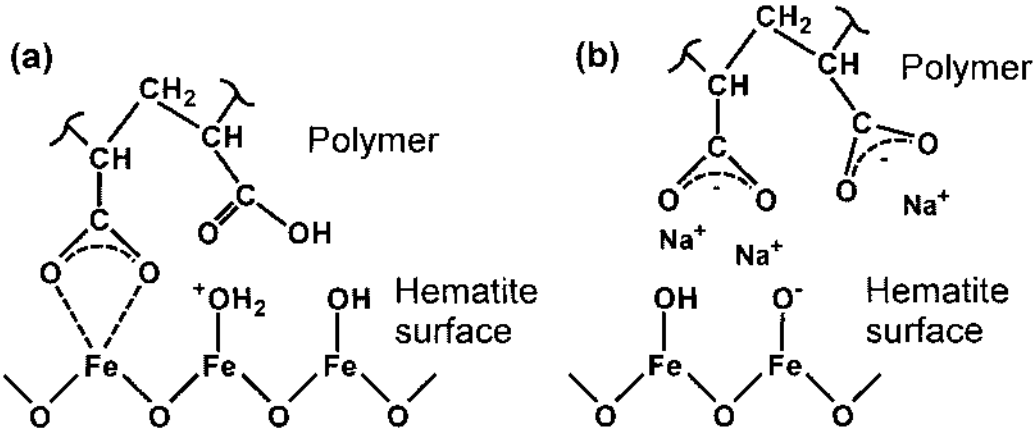


Figure 5 — Schematic representation of the proposed adsorption mechanism of polyacrylate onto hematite at (a) pH 2 and (b) pH 13 at high ionic strength.

likely is an electrostatic adsorption process as shown in Figure 5b, with adsorption of the polymer's anionic functionalities to the negatively charged hematite surface facilitated by charge neutralisation through sodium cations.

Adsorption was found to be irreversible at both the low and high pH conditions described above, with the polymer not removed to any significant degree by extended washing with polymer-free electrolyte or water. While the individual electrostatic surface binding as shown in Figure 5b may be weak, multiple bonding along a polymer chain provides the observed irreversibility.

### **3.3** *Effect of electrolyte (NaCl) at high pH*

As a consequence of the irreversible nature of the polymer adsorption, it was not possible to use the same hematite film for more than one measurement. Considerable effort was therefore made to achieve reproducible casting of the film onto the ATR crystal, ensuring a consistent available surface area of hematite. This allowed the effect of changing solution conditions on the extent of polyacrylate adsorption to be effectively quantified. Solutions of PAA13M (50 ppm) were flowed at a constant rate across the hematite colloid at pH 13 for a range in electrolyte concentrations (0.1 to 3 M NaCl). Figure 6a shows the integral of the peak for the asymmetric stretch of the carboxylate ion (1560 $cm^{-1}$) as a function of time. The plateau adsorption values at each electrolyte concentration are given in Figure 6b. The extent of polymer adsorption increased with the electrolyte concentration up to approximately 1 M NaCl. This may indicate that monolayer adsorption was achieved.

Figure 7a shows the zeta potential of the hematite colloid measured as a function of pH. Over most of the pH range the zeta potential was positive, with the iso-electric point (iep) at a pH of approximately 10. Literature values for the iep of hematite have been reported in the range 2 to 10, although values below 7 are usually attributed to impurities such as silicate, typically found in naturally occurring hematites. For synthetic hematite iep values generally lie between 8 and 9. At pH values above the iep the zeta potential became increasingly negative, achieving a minimum of -45 mV at pH 11.9. The subsequent rise in zeta potential at higher pH values may be attributed to the increase in ionic strength.

The effect of ionic strength on the measured zeta potential is clearly demonstrated in Figure 7b. As the added electrolyte concentration was raised to 0.3 M the magnitude of the zeta potential approached zero, leading the colloidal suspensions to destabilise and aggregate. For 1.0 M of added electrolyte the apparent zeta potential became positive (+74 mV), increasing further in magnitude for 2.9 M electrolyte (180 mV). This implies that $Na^+$ ions are specifically

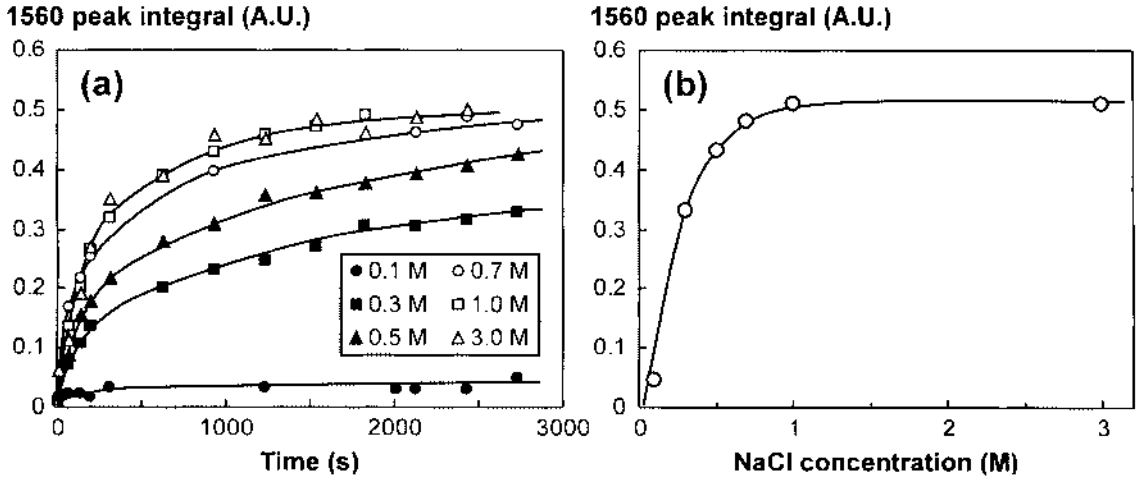


Figure 6 — Adsorption of 50 ppm PAA13M onto hematite at pH 13, (a) asymmetric carboxylate stretch as a function of reaction time, and (b) plateau adsorption as a function of NaCl concentration.

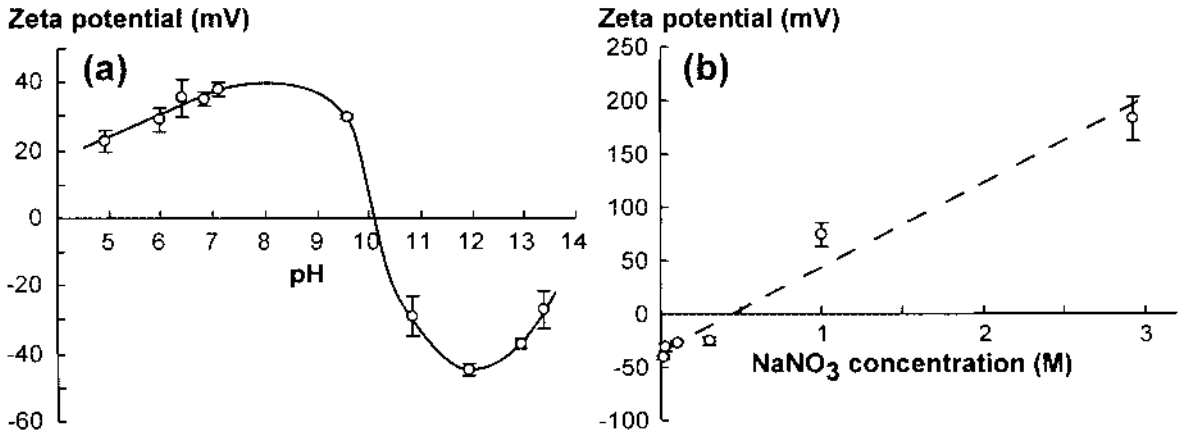


Figure 7 — Zeta potential of the hematite colloid (a) measured as a function of pH, and (b) at pH 13 measured as a function of $NaNO_3$ concentration.

adsorbed on the hematite surface, to the point that at very high salt concentrations such adsorption leads to the surface becoming positively charged. Positive potentials was also observed by Rowlands et al. for AcoustoSizer measurements on aluminium hydroxide particles in 3 M NaCl. They attributed the shift to positive charge to the sodium ion being more strongly adsorbed on the surface than chloride.

The magnitude of these measured zeta potentials should be viewed with significant caution, as the structure of the double layer at such high ionic strengths is poorly understood. Under these conditions the colloids were observed to aggregate, suggesting that despite the high charge at the shear plane (i.e. a high zeta potential), the high concentration of solution cations and anions prevents the particle dispersion that would be expected at low ionic strength, based on DLVO theory.

The above results are consistent with the polyacrylate adsorption observations from Figure 6. At pH 13 in the absence of added electrolyte the negative surface charge of hematite prevents adsorption of the negatively charged polymer. With 0.3 M salt the overall charge is reduced sufficiently to allow some positive sites to exist on the surface, thus enabling adsorption as shown in Figure 5b. Higher salt concentrations ensure the majority of surface sites are at least neutral, and polymer adsorption approaches a plateau level.

### **3.4** *Effect of cation type on adsorption at high pH*

If the solution cation plays a critical role in the adsorption of polyacrylates, then changing the identity of the cation may have an effect on the process. Figure 8 compares the adsorption of PAA450K at pH 13 with either 0.20 M lithium, sodium or cesium salts. The presence of lithium enhanced adsorption to the greatest extent, while cesium gave the weakest enhancement. Such behaviour may either be attributed to the effect of the cation on surface charge, or to the ability of the cation to shield the negative charge of the polymer functionalities, thereby influencing the polyelectrolyte's solution dimensions. However, it was found from MALLS that the radius of gyration of PAA450K in each electrolyte was 155±12 nm, independent of the solution cation. This was consistent with the results of Boisvert et al., who used osmotic pressure measurements to show that the interaction of monovalent cations and polyacrylate was non-specific across the pH range 4 to 9.

The effect of the solution cation on the zeta potential for hematite was examined at pH 12, as this pH provided the most negative potential for the colloid in the absence of added salt (Figure 7a). Figure 9 shows the measured zeta potentials as a function of electrolyte concentration, using either $LiNO_3$ or $NaNO_3$. As was the case at pH 13, the introduction of an electrolyte decreased the magnitude of the negative potential, and at high concentrations substantial

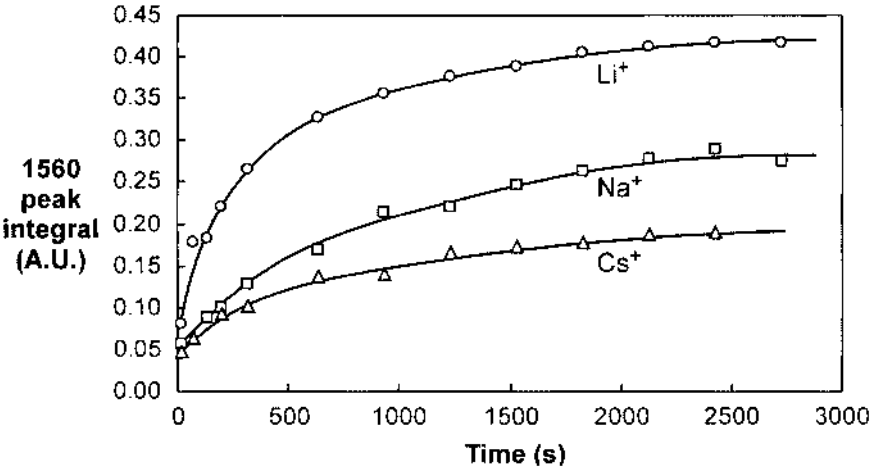


Figure 8 — Adsorption of PAA450K (50 ppm) at pH 13 (made up in LiOH, NaOH or CsOH) with a 0.2 M electrolyte concentration (LiCl, NaCl or CsCl) monitored by the integral of the 1560 $cm^{-1}$ peak.

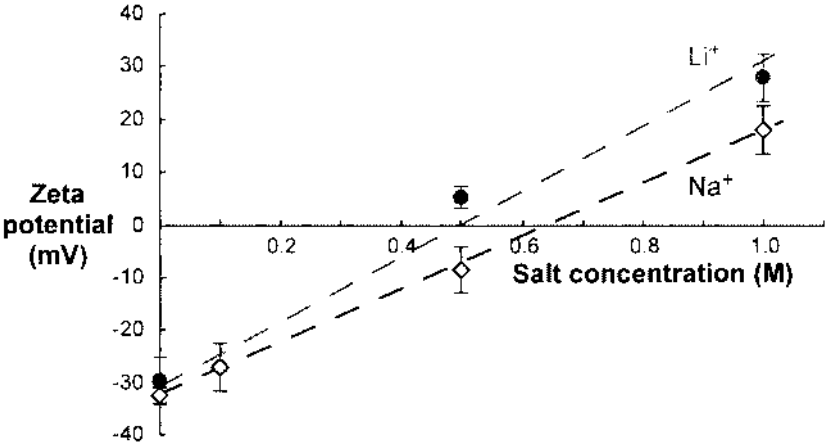


Figure 9 — Hematite zeta potential at pH 12 as a function of $LiNO_3$ or $NaNO_3$ concentration.

positive potentials were measured. The results suggest the lithium cation has a stronger specific interaction with hematite than sodium, with the zeta potential approaching zero at approximately 0.50 and 0.65 M for $LiNO_3$ and $NaNO_3$, respectively. The order obtained for attractive interactions between surface and counter-ion of $Li^+ > Na^+ > Cs^+$ is the reverse of that expected from classical theory. Sodium is generally expected to have a greater attraction to the negative hematite surface than the lithium ions as a consequence of its smaller radius of hydration allowing closer approach to the surface.

However, there are studies that support the order observed here. Breeuwsma and Lyklema used surface charge measurements on a synthetic hematite to show affinity for the hematite surface in the order $Li^+ > K^+ = Cs^+$ at pH values above that of the pzc. They attributed this to dehydration of the lithium cation but were unable to describe why this would only occur in selected systems.

Rutile ($TiO_2$) is similar to hematite in that the surface hydrates quite readily. In their explanation of the preferred affinity of $Li^+$ to the rutile surface, Berube and de Bruyn observed an inverse lyotropic adsorption sequence ($Li^+ > Na^+ > K^+ > Cs^+$) on rutile, which they described with a 'structure making-structure breaking' model. Water molecules associated with surfaces like hematite or rutile exhibit a high degree of order and structure (structure making). The addition of large ions (e.g. $Cs^+$) that are not heavily hydrated tends to destroy the way in which water molecules cluster. In contrast, small and heavily hydrated ions (e.g. $Li^+$, $Na^+$) may be incorporated into the water structure with minimal disruption, and are therefore more likely to be specifically adsorbed. Whether an oxide surface is structure making or breaking can be predicted from the pzc and the oxide's heat of immersion.

### **3.5** *Other information*

Full quantification of polymer adsorption required further characterisation of the cast hematite film and detailed analysis of the depth of penetration for the sampling infrared evanescent wave. This has allowed the determination of adsorption isotherms and adsorption densities from FTIR-ATR for different polymer products. In addition to such equilibrium data, these experiments provide adsorbed polymer peak areas as a function of time for different solution conditions and with different molecular weight polymers. It is anticipated that the derived kinetic information will ultimately be incorporated in modelling of bauxite residue aggregation processes.

## 4 Summary

As an *in situ* technique, FTIR-ATR avoids the inevitable binding changes associated with *ex situ* sample preparation and yields information that is essentially restricted to the solid-liquid interface. Its application to polyacrylate adsorption on hematite has provided the first direct evidence of how such polymers adsorb at high pH and the critical role of the solution cation. This has been supported by zeta potential measurements at high ionic strength.

Procedures have now been established for quantification of the adsorption kinetics and isotherms by FTIR-ATR. Future work will include the comparison of polyacrylate versus hydroxamate adsorption on hematite, and an investigation of flocculant adsorption on colloidal gibbsite is also planned.

## Acknowledgements

This research has been supported by the Australian Government's Cooperative Research Centre (CRC) program, through the AJ Parker CRC for Hydrometallurgy. This support is gratefully acknowledged. One of us (L.J. Kirwan) is grateful for the support of an Australian Postgraduate Award from the ARC through the Curtin University of Technology.

## REFERENCES

**Jones, F., Farrow, J.B. and van Bronswijk, W.**, Flocculation of haematite in synthetic Bayer liquors, *Colloids Surf. A: Physicochem. Eng. Aspects*, 135, 183–192 (1998).

**Jones, F., Farrow, J.B. and van Bronswijk, W.**, Effect of caustic and carbonate on the flocculation of haematite in synthetic Bayer liquors, *Colloids Surf. A: Physicochem. Eng. Aspects*, 142, 65–73 (1998).

**Farrow, J., Jones, F. and van Bronswijk, W.**, Hematite flocculation under Bayer conditions, *5th International Alumina Quality Workshop*, Bunbury, 21-26 March, 1999, 466–477.

**Bremmell, K.E., Scales, P.J. and Healy, T.W.**, The role of chemical flocculants in the disposal of red mud, *5th International Alumina Quality Workshop*, Bunbury, 21-26 March, 1999, 489–497.

**Jones, F., Farrow, J.B. and van Bronswijk, W.**, An infrared study of a polyacrylate flocculant adsorbed on hematite, *Langmuir*, 14, 6512–6517 (1998).

**Sperline, R. and Freiser, H.**, Infrared attenuated total reflection spectroscopy of surface active species, In *The Handbook of Surface Imaging and Visualization*, (Ed. Hubbard, A.T.), CRC Press, Boca Raton, Florida, 245–263 (1995).

**Hind, A.R., Bhargava, S.K. and Grocott, S.C.**, Attenuated total reflection Fourier transform infrared spectroscopic investigation of the solid/aqueous interface of low surface area, water-soluble solids in high ionic strength, highly alkaline, aqueous media, *Langmuir*, 13, 3483–3487 (1997).

**Hind, A.R. and Bhargava, S.K.**, The adsorption of sodium oxalate stabilisers to the surface of gibbsite (a Bayer Process solid) under high ionic strength, high pH conditions, *Light Metals*, 65–70 (2000).

**Allara D.L. and Nuzzo, R.G.**, Spontaneously organized molecular assemblies. 2. Quantitative infrared spectroscopic determination of equilibrium structures of solution-adsorbed *n*-alkanoic acids on an oxidised aluminium surface, *Langmuir*, 1, 52–66 (1985).

**Lee, D.H., Condrate, R.A. and Reed, J.S.**, Infrared spectral investigation of polyacrylate adsorption on alumina, *J. Materials Sci*., 31, 471–478 (1996).

**Kan, S., Yu, S., Peng, X., Zhang, X., Li, D., Xiao, L., Zou, G. and Li, T.**, Formation process of nanometer-sized cubic ferric oxide single crystals, *J. Colloid Interface Sci.*, 178, 673–680 (1996).

**Tscharnuter, W.**, Mobility measurements by phase analysis, *Applied Optics*, 40, 3995–4003 (2001).

**Deacon, G.B. and Phillips, R.J.**, Relationships between the carbon-oxygen stretching frequencies of carboxylato complexes and the type of carboxylate coordination, *Coordination Chemistry Reviews*, 33, 227–250 (1980).

**Pugh, R.J. and Lundström, H.**, In *Flocculation in Biotechnology and Separation Systems*, (Ed. Attia, Y.A.), Elsevier, Amsterdam, 673–694 (1987).

**Rowlands, W.N., O'Brian, R.W., Hunter, R.J. and Patrick, V.**, Surface properties of aluminium hrdroxide at high salt concentrations, *J. Colloid Interface Sci.*, 188, 325–335 (1997).

**Boisvert, J.-P., Malgat, A., Pochard, I. and Daneault, C.**, Influence of the counter-ion on the effective charge of polyacrylic acid in dilute conditions, *Polymer*, 43, 141–148 (2002).

**Breeuwsma, A. and Lyklema, J.**, Interfacial electrochemistry of haematite ($\alpha$-$Fe_2O_3$), *Discussions of the Faraday Society*, 52, 324–333 (1971).

**Berube, Y.G. and de Bruyn, P.L.**, Adsorption at the rutile-solution interface. II. Model of the electrochemical double layer, *J. Colloid Interface Sci.*, 28, 92–105 (1968).

**Dumont, F., Van Tan, D. and Watillon, A.**, Study of ferric oxide hydrosols from electrophoresis, coagulation, and peptization measurements, *J. Colloid Interface Sci.*, 55, 678–687 (1976).

**Kirwan, L., van Bronswijk, W and Fawell, P.**, An in situ FTIR-HATR investigation of the adsorption of polyacrylic acid onto hematite, *4th Australian Conference on Vibrational Spectroscopy*, 9–11 July 2001, Brisbane.